ADVANCES IN OFFSHORE AND ONSHORE ANCHORING SOLUTIONS

C. Gaudin[1], C.D. O'Loughlin[1], M.F. Randolph[1], M.J. Cassidy[1], D. Wang[1], Y. Tian[1], J.P. Hambleton[2], R.S. Merifield[2,3]

[1]*ARC Centre of Excellence for Geotechnical Science and Engineering, The University of Western Australia, Crawley, WA, Australia*
[2]*ARC Centre of Excellence for Geotechnical Science and Engineering, The University of Newcastle, Callaghan, NSW, Australia*
[3]*SMEC, Newcastle, NSW, Australia*

ABSTRACT

The paper presents a snapshot of the research performed within the ARC Centre for Geotechnical Science and Engineering (CGSE) on anchoring systems. The focus is on the determination of nominal bearing factors and the performance of three different types of anchors: the suction embedded plate anchor, the dynamically embedded plate anchor and the helical anchor. The paper emphasises the wide range of analytical, numerical and physical modelling techniques developed within the CGSE to (i) develop a rigorous understanding of the soil-anchor interaction and (ii) create practical tools that can be readily used for design.

1 INTRODUCTION

Anchors are commonly used onshore and offshore as foundation systems for structures that required uplift resistance (either vertical or inclined). These include floating offshore platforms, buried pipelines, floating renewable energy devices, transmission towers and sheet pile walls. Offshore and onshore anchors vary widely in shape, size, mode of installation and usage, but they all raise the same challenges: (i) establishing undrained bearing capacity factors under monotonic loading as a function of the anchor shape and geometry and (ii) establishing the relevant soil strength parameters to determine the ultimate capacity. The latter point is complicated by the necessity to account for specific characteristics of the soil (e.g., softening and strain-rate effects), potential changes in soil characteristics generated by installation (and potential setup after installation) and the nature of the loading, which can be cyclic or sustained over a long period.

The CGSE has been actively engaged in research on anchoring systems since its inception, building on the internationally recognised expertise achieved by the Centre for offshore Foundation Systems at The University of Western Australia and the Centre for Geotechnical and Materials Modelling at The University of Newcastle. The synergies created by the CGSE have been instrumental in investigating new research areas, notably associated with the installation of anchors for both offshore and onshore applications. The paper reviews the research undertaken over the last decade, focusing on establishing nominal bearing capacity factors, extensive research performed on two particular types of offshore anchor (the suction embedded plate anchor and the dynamically embedded plate anchor), and the development of a design framework for helical anchors (multi-plate anchoring systems).

2 BEARING CAPACITY FACTORS

2.1 BEARING CAPACITY IN CLAY

The bearing capacity of anchors deeply embedded in clay may be expressed in terms of a bearing capacity factor $N_c = F_{max}/As_{u0}$, where F_{max} is the maximum force that can be sustained normal to a centrally loaded plate of area A. The undrained shear strength, s_{u0}, is regarded as the average shear strength at the anchor centroid, allowing for variation of the shear strength with depth. Evaluation of the bearing factor needs to consider whether the soil remains bounded at the base of the anchor during pull-out. This separates the solutions into breakaway cases, where tensile stresses due to suction cannot be sustained at the anchor base, and no breakaway cases, where suction is developed and sustained. The latter case is relevant for deeply embedded anchor under undrained conditions and is of more practical interest.

For plate anchors with simple geometries, Merifield *et al.* (2001, 2003, 2005) established a comprehensive set of lower and upper bound solutions for bearing capacity factors with no breakaway as a function of anchor shape, roughness, embedment depth, overburden pressure and anchor inclination. Solutions were further refined using both lower bound and upper bound plasticity theorems (Martin and Randolph, 2001) and large deformation finite element analysis (Wang *et al.*, 2010a, amongst others).

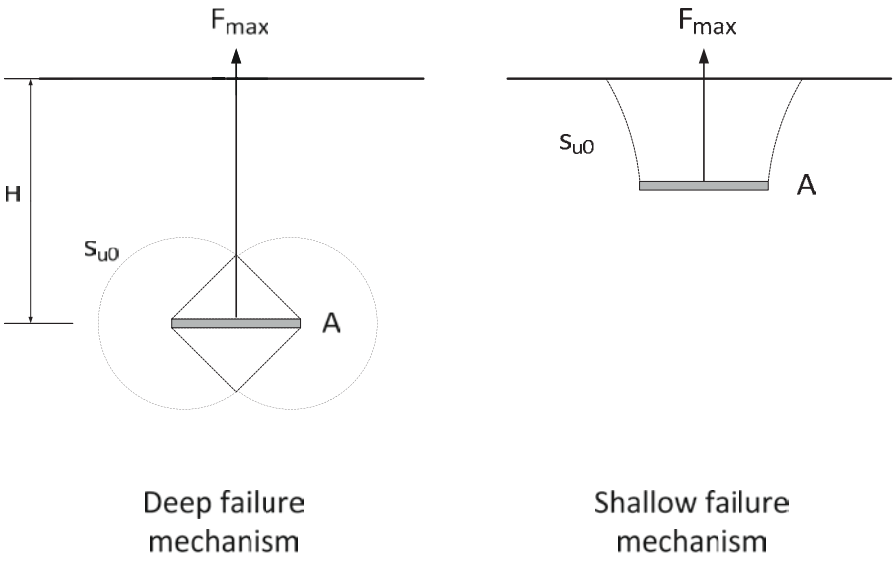

Figure 1: Anchor failure mechanism under no breakaway (deep) and breakaway (shallow) conditions.

For a vanishingly thin circular plate deeply embedded in uniform soil, with the soil remaining bonded to the plate base, a symmetrical flow-around mechanism is generated (Figure 1) and the exact uplift capacity factors for fully smooth and rough surfaces are 12.42 and 13.11, respectively (Martin and Randolph, 2001). Finite element solutions for a square plate with thickness t = 0.05 B (Elkhatib, 2006) yield values of 12.5 (smooth) and 13.5 (rough). Comparable analyses for a rectangular plate give uplift capacity factors that vary from 12.0 to 11.6 (smooth) and 12.5 to 11.9 (rough) as the aspect ratio changes from $L/B = 2$ to 6, adjusting the values by Wang et al. (2010a) for the level of mesh refinement. For the rectangular plate, the bearing capacity factors decrease with increasing aspect ratio and tend toward the value for a strip anchor. Finite element solutions show that an increase in anchor thickness results in a slight increase in the bearing capacity factor. For example, the increase is less than 6% in the case of a rough plate with t/B increasing from 0.05 to 0.14 (Elkhatib, 2006).

The large deformation finite element (LDFE) approach was also used extensively to extend the analytical solutions to various shapes of anchors. Song *et al*. (2008) and Wang *et al*. (2010a) investigated the pull-out process for strip and rectangular plates of width B under both breakaway and no breakaway conditions. Under no breakaway conditions, the bearing capacity factor increases sharply with embedment depth until the maximum capacity is achieved at an embedment ratio of $H/B = 2$. At any depth, the capacity under no breakaway conditions constitutes an upper limit on the capacity for breakaway conditions.

Nominal bearing capacity factors are now well established for a wide range of anchor configurations and embedment. There are, however, many other considerations that may affect bearing factors and that need to be considered for design. With respect to the anchor geometry, the presence of a shank on the anchor (which is typically used to connect the anchor to the loading line) may increase the size of the failure mechanism by extending the volume of material that remains rigidly attached to the plate.

Nominal bearing capacity factors may be used to calculate the ideal anchor bearing capacity under monotonic loading, based on the local undrained shear strength. Depending on the rate of loading and the magnitude of strains generated, the shear strength may need to be corrected to account for rate and softening effects. Rate effects typically increase the undrained shear strength of clay by 15-20% per log increase in pulling rate. In contrast, strain softening may reduce the strength by up to 17%). Strain softening can cause the anchor to undergo substantial displacement before mobilising its full bearing capacity. The keying process, described further in Section 3.1, is an example where softening has a significant effect.

2.2 BEARING CAPACITY IN SAND

The determination of bearing capacity factors in sand is a more complex operation and, accordingly, there are no widely-accepted solutions. Bearing capacity factors in sand may be expressed as $N_\gamma = F_{max}/\gamma HA$, where γ is the unit weight of the soil and H is the embedment depth. Somewhat unsurprisingly, bearing factors established from centrifuge model tests, 1g small-scale model tests and pressure chamber or full-scale *in situ* tests exhibit relatively large scatter, preventing the establishment of a universal solution. Finite element analysis also proves to be challenging, owing to the difficulty in developing a constitutive soil model that accounts for the specific behaviour of sand, namely post peak friction and dilation.

Merifield and Sloan (2006) and Merifield *et al.* (2006) established bearing capacity factors for strip, square and circular plate anchors in sand using finite element limit analysis. Whilst the solutions may be used to provide a first estimate of the anchor capacity, they need to be used carefully, since the assumption of associativity (identical friction and dilation angle) likely overestimates the real capacity. Work is currently in progress within the CGSE to develop a robust and reliable sand model for large deformation finite element analysis.

3 SUCTION EMBEDDED PLATE ANCHOR

3.1 INTRODUCTION

The suction embedded plate anchor (SEPLA) is an efficient and economical anchoring solution developed to moor large floating facilities on soft seabeds (Wilde *et al.*, 2001, Ehlers *et al.*, 2004). The SEPLA consists of a thin fluke, a shank connecting the fluke to a padeye (i.e. the loading point) and a full-length keying flap hinged to the top of the fluke (Figure 2). A suction caisson, termed the follower, is used to install the plate anchor to its design embedment depth (Dove *et al.*, 1998). Prior to 2004, SEPLA field application was limited to temporary moorings for mobile offshore drilling units (MODUs). The first permanent application occurred in 2006 for a Floating Production Unit in the Gulf of Mexico.

A large body of research has been undertaken over the last 10 years within COFS and more recently within the CGSE to investigate the performance of SEPLAs for both temporary and permanent loading. The work focused first on characterising the keying process and predicting with simple analytical tools the resulting loss of embedment. Subsequent research focused on monotonic capacity, accounting for the loss of embedment, the load inclination and more specifically for the geometrical features of SEPLAs, including the keying flap and the position of the loading point. Research currently in progress includes the behaviour of SEPLAs under sustained and cyclic loading.

The development of all these aspects has greatly benefited from the wide range of modelling techniques developed within the CGSE. These include (i) state-of-the-art centrifuge modelling and associated analyses based on particle image velocimetry, (ii) total stress large deformation finite element analysis and (iii) effective stress coupled finite element analysis. The main outcomes of this research and collaboration within the CGSE are summarised in the following sections.

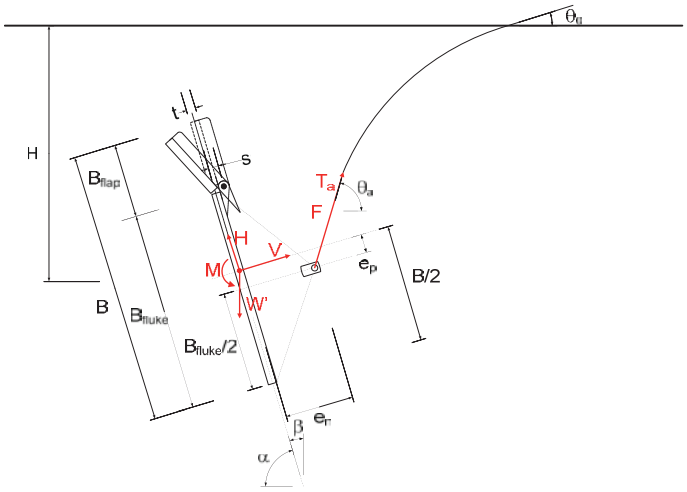

Figure 2: Schematic of a suction embedded plate anchor (SEPLA).

3.2 KEYING

The challenge in estimating anchor capacity is more in prediction of the keyed embedment than in estimating the bearing capacity factor, which numerical and experimental analysis has shown to be in the range of N_c = 11 to 12 for deeply embedded rectangular anchors, as discussed in Section 2. In typical seabeds with strength increasing almost proportionally with depth, the loss of embedment during keying may result in a reduction in capacity of up to 20 %.

Loss of embedment during keying has been extensively investigated, both experimentally (O'Loughlin *et al.*, 2006; Song *et al.*, 2009) and numerically using large deformation finite element (LDFE) analysis (Song *et al.*, 2008; Wang *et al.*, 2010a). The latter notably included the anchor-chain interaction, adjusting the load inclination at the padeye as the chain is tensioned.

Numerical results, validated by experimental data, show the importance in soft soil of the padeye eccentricity, e_n, the anchor thickness, t, and the buoyant weight of the anchor, W'. These variables influence the moment loading on the

anchor, *M*, particularly prior to the point where the vertical component of load balances the anchor weight. A large moment encourages rotation of the anchor instead of vertical motion, thus reducing the embedment loss.

Predictions of the loss of embedment have been established by Wang *et al*. (2011) based on large deformation finite element analysis, considering the relevant non-dimensional groups of the anchor and soil parameters. For typical SEPLA weights and geometry, the loss of embedment under vertical pull-out was found to range from 0.6 to 1 times the anchor height, which is in good agreement with experimental data (O'Loughlin *et al*., 2006) but in the lower range of data from field trials (Wilde *et al*., 2001). SEPLAs are typically loaded at an inclination of around 40 degrees from horizontal at the mudline. The influence of the load inclination on the loss of embedment has been investigated numerically (Wang *et al*., 2011) and experimentally (Gaudin *et al.,* 2008, 2010). In all cases, the loss of embedment was found to decrease linearly with the reduction of load inclination to the horizontal. For typical loading conditions, this effect promotes a reduction in the loss of embedment, which becomes 0.4 to 0.6 times the anchor height.

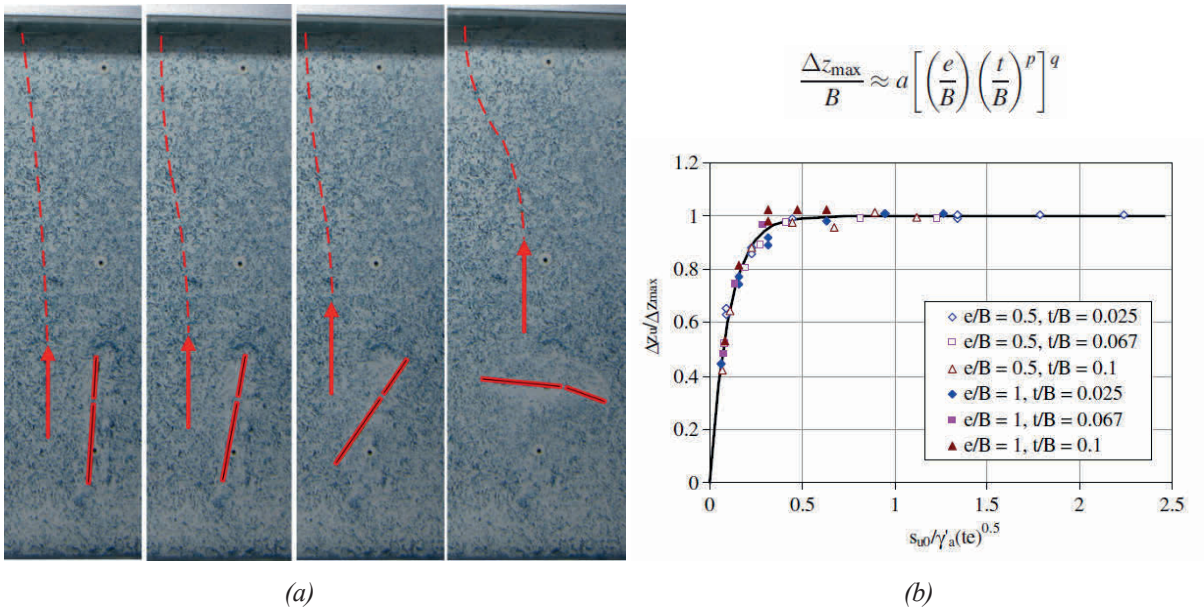

(a) *(b)*

Figure 3: (a) SEPLA motion during pull-out in a centrifuge test with soft normally consolidated clay. Illustration of the keying process and associated loss of embedment, after Gaudin *et al*., 2008 (b). Quantification of the loss of embedment under vertical pull-out, after Wang *et al.* (2011).

3.3 MONOTONIC CAPACITY

The monotonic pull-out capacity of a 'wished in place' plate anchor is well established, as discussed in Section 2. However, for design purposes, it is more suitable to determine a bearing capacity factor that accounts for (i) the loss of embedment during keying, which effectively leads to a reduction in the soil's strength under typical conditions and (ii) particularity of the SEPLA geometry when compared to an ideal rectangular plate anchor.

SEPLAs often feature a keying flap in order to limit the vertical displacement of the anchor during keying and hence the potential loss of embedment (Figure 2). The keying flap is a solid plate attached to the top of the anchor, which is free to rotate a limited amount (about 20°) away from the shank but restrained from rotating towards the shank. Early field tests incorporated the flap with the aim of "*[increasing] the vertical bearing area of the SEPLA and preventing it from moving back up its installation track when tensioned*" (Wilde *et al*., 2001). As the anchor moves upwards during keying, the shearing forces acting along the flap are expected to rotate the flap away from the shank, providing extra bearing resistance against vertical displacements and consequently reducing the loss of embedment. A by-product of the keying flap is the development of a loading offset, e_p, as the padeye is moved below the anchor's centroid (see Figure 2). Both the flap performance and the effect of the loading offset on the anchor trajectory and capacity have been investigated extensively via physical and numerical modelling.

Visual observations from centrifuge tests (Gaudin *et al*., 2008) showed that the keying flap does not rotate during keying as intended. The shearing forces rotating the flap are overcome by the normal forces acting at the back of the flap as the anchor rotates, locking the flap in place, as illustrated in Figure 3. Numerical analyses (Wang *et al*., 2013a; Tian *et al*., 2013) validated the experimental observations and provided further insights into the motion of the flap. Most noteworthy is the non-rotation of the flap during keying for loading inclination θ_a greater than 50° (which is typically the case), but the activation of the flap post-keying when the anchor experiences translation along the loading direction reduces the projected area of the anchor and alters the flow of soil around the anchor. The combination of

these two aspects results in a reduction of the anchor capacity and the associated bearing capacity factor. However, this reduction is balanced by a reduction in the loss of embedment during keying, which results not from the rotation of the keying flap but from the loading offset. The mechanism by which the offset reduces the loss of embedment is identical to that involved with respect to loading eccentricity. By increasing the loading offset, the moment acting at the centroid of the anchor is augmented, resulting in a higher rotation rate of the anchor with respect to the horizontal displacement. Further investigations performed by Tian *et al.* (2014a) indicated that the load eccentricity plays a more important role than the load offset, but both can be combined to predict the loss of embedment, thus updating the formulation initially developed by Wang *et al.* (2011).

Evidently, the detrimental effect of reduction in the bearing capacity factor with increasing loading offset balances the beneficial effect of reduction in loss of embedment. The latter depends on the soil strength gradient, or more specifically the strength ratio kB/s_{ui}, where s_{ui} is the shear strength at the anchor centroid at the initial embedment. The benefit from a reduction in loss of embedment increases with increasing kB/s_{ui}. Both effects can be combined by defining an operative bearing capacity factor, N_{op}, that depends on s_{ui} rather than s_{u0} and include all aspects of the anchor's geometry and behaviour. Figure 4 presents the evolution of N_{op} as a function of the offset ratio η for strength ratios ranging from kB/s_{ui} = 0 to 1.5 and an eccentricity ratio of e_n/B = 0.5. This is the bearing factor that should be used for design as it is based on a known constant shear strength value. Detailed results for e_n/B = 0.5 and 1 are presented by Tian *et al.* (2014a).

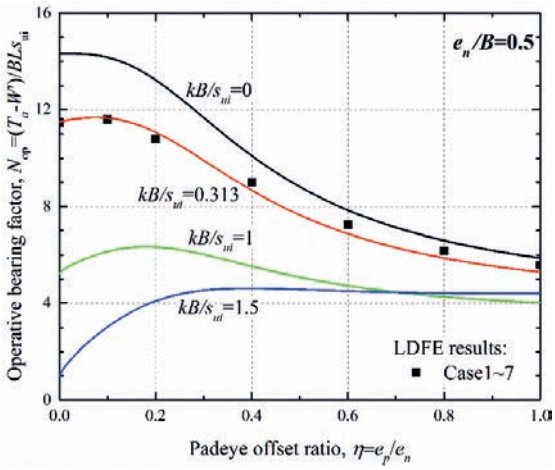

Figure 4: Establishment of optimal operative bearing capacity factor N_{op} for different offset and strength ratios.

For a nil stress ratio, the best performance is evidently achieved without loading offset since there is no benefit in reducing the loss of embedment. As the strength ratio increases, the curves exhibit a peak capacity, enabling identification of an optimal offset ratio η. The peak occurs for higher values of offset ratio as the strength ratio increases, and occurs for $\eta \approx$ 0.1 at typical strength ratios of kB/s_{ui} = 0.2 to 0.3. This value is close to current design practice, albeit arising from an incorrectly designed keying flap.

The most important outcome of the analyses relates to the values of operative bearing factor N_{op}, which can be reduced to values as low as ~11.5 for kB/s_{ui} = 0.313, or even to ~4.5 for the extreme strength ratio of kB/s_{ui} = 1.5. For high strength ratios, the padeye offset mitigates the effect of loss of embedment during keying by a small margin (i.e. higher operative bearing capacity factors are achieved than with no loading offset) but overall causes a significant reduction to the operative bearing capacity factor. These results cover a wide range of theoretical cases. In practice, the strength ratio is typically within the range kB/s_{ui} = 0 to 0.3. In addition, as discussed briefly in the following section, anchors with offset ratios of η = 0.2 to 0.3 exhibit a tendency to dive into deeper soil, leading to an increase in capacity. Thus, operative bearing capacity factors lower than ~10 are not believed to be relevant for design.

These observations have prompted additional research to try to develop a redesign of the SEPLA that would both reduce the loss of embedment during keying and achieve a higher bearing capacity factor. A first idea is to reverse the keying flap, allowing rotation towards the shank rather than away from the shank. This concept was tested by Tian *et al.* (2014b) using finite element analysis. Preliminary results varying the length of the flap indicated that an increase of about 20% compared to the current design could be achieved.

While complex finite element analysis and centrifuge modelling are necessary to develop a comprehensive understanding of the anchor behaviour, they are not necessarily suitable for routine design. In collaboration with ExxonMobil, a practical design tool has been developed based on the plasticity framework and implemented into an Excel™ spreadsheet (Cassidy *et al.*, 2012). The model assumes rigid plasticity and defines combined normal, sliding and rotational yield envelopes from which the anchor displacement can be inferred from any load path reaching the

envelopes from a plastic potential with an associated flow. The model was validated against numerical and experimental data and enables prediction of the anchor trajectory and capacity during keying and after mobilisation of the peak capacity. Another advantage of the plasticity approach is the ability to conduct sensitivity studies, especially with respect to the anchor's geometry and soil conditions. Recently completed studies confirm the important role of the loading offset and strength gradient on the loss of embedment and subsequent capacity, but also reveal the ability of the SEPLA to dive into deeper and stronger soils under specific load offset and inclination. This was further investigated numerically by Tian *et al*., (2014c), who demonstrated that anchor diving occurs only for load inclination θ_a lower than 70° and that the optimal offset ratio e_p/e_n is approximately 0.3. In this study, the load inclination θ_a was taken to remain constant. In reality, this angle varies depending on motion of the chain within the soil. Further studies are being carried out to predict the possible ultimate embedment depth and corresponding holding capacity, considering the motion of the chain.

3.4 SUSTAINED AND CYCLIC LOADING

SEPLAs have been commonly used over the last decade for temporary facilities, anchoring MODUs. The use of SEPLAs for permanent facilities was first considered by ExxonMobil for a development in West Africa. This consideration raised concerns associated with the long-term performance of the anchor against sustained loading, generated by tides and seasonal currents. Wong *et al.* (2012) reported centrifuge tests on a 1/150th scaled rectangular SEPLA, where various conditions of monotonic, sustained and cyclic loading were examined. Results indicated that the level of loading, T_{sus}/T_{max}, that could be sustained indefinitely was about 85% of the monotonic ultimate capacity T_{max} (Figure 5). Above that level, accumulation of anchor displacements eventually led to anchor failure. Failure was associated with creep (i.e. reduced shear strength of the soil at low strain rates), which overcomes the enhancement of soil strength and anchor capacity resulting from consolidation occurring during sustained loading. The benefit from consolidation is evident for levels of loading, T_{sus}/T_{max}, lower than 85%, with an increase in post sustained loading capacity T_{max}-$_{sus}/T_{max}$, of up to 1.9 times the initial capacity (see Figure 5).

Under cyclic loading, similar mechanisms occur as for sustained loading, with some additional damage from cyclic loading. Model tests covering a variety of cyclic loading ranges (mean loads from 35 to 58% of the monotonic capacity and peak loads from 53 to 90% of the monotonic capacity) showed that failure occurred for any loading where the peak load exceeded 75% of the monotonic capacity.

Further insights into the behaviour of plate anchors under sustained loading has been provided by Han *et al.* (2015) who performed a series of centrifuge tests using particle image velocimetry techniques to capture the soil flow mechanism around the anchor during sustained loading. The tests confirmed the threshold beyond which failure occurred under sustained loading and revealed the conditions generating breakaway at the anchor invert. Under low levels of sustained loading, the anchor displacement rate at the end of the consolidation process generates drained conditions and the anchor invert remains bonded to the soil. Under higher levels of sustained loading (that do not generate failure), the anchor displacement rate at the end of the consolidation process still generates undrained conditions. However, consolidation (swelling) behind the anchor is faster and ends before that ahead of the anchor. This results in the effective stresses behind the anchor reducing to zero, so tensile stresses can no longer be sustained. Breakaway occurs without a reduction in anchor capacity since the soil ahead of the anchor has consolidated, increasing its strength and developing a higher resistance.

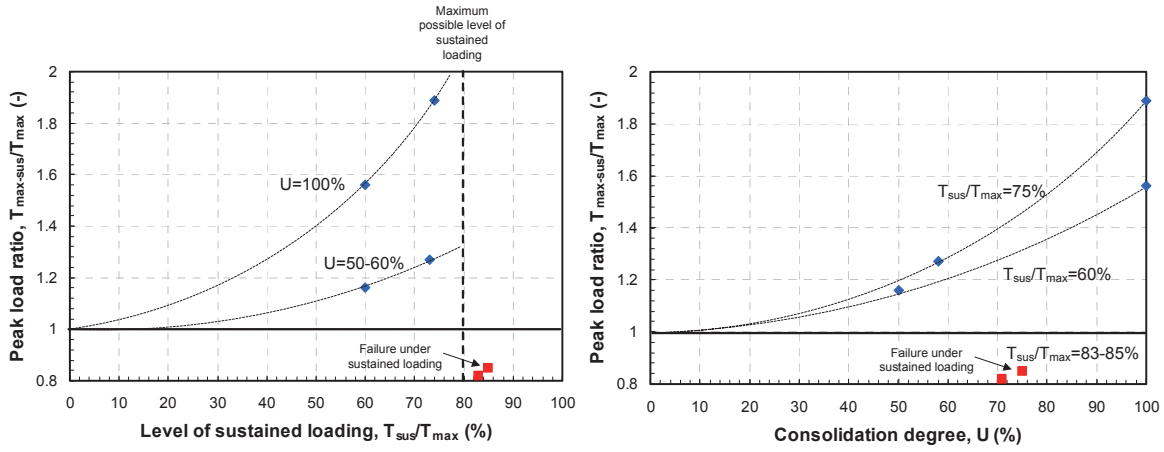

(a) *(b)*

Figure 5. Increase in anchor capacity following sustained loading (a) as a function of the level of sustained loading and (b) as a function of the degree of consolidation.

4 DYNAMICALLY EMBEDDED PLATE ANCHOR (DEPLA)

4.1 CONCEPT

The dynamically embedded plate anchor (DEPLA) is a new dynamically installed anchor concept that combines the installation benefits of dynamically installed anchors with the capacity benefits of plate anchors. The DEPLA comprises a removable central shaft or 'follower' that may be fully or partially solid and a set of four flukes (see Figure 6).

A stop cap at the upper end of the follower prevents it from falling through the DEPLA sleeve and a shear pin connects the flukes to the follower. As with other dynamically installed anchors, the DEPLA penetrates to a target depth in the seabed by the kinetic energy obtained through free-fall. After embedment the follower line is tensioned, which causes the shear pin to part allowing the follower to be retrieved for the next installation, whilst leaving the anchor flukes vertically embedded in the seabed. The embedded anchor flukes constitute the load bearing element as a plate anchor. A mooring line attached to the embedded flukes is then tensioned, causing the flukes to rotate or 'key' to an orientation that is normal or near normal to the direction of loading. In this way, the maximum projected area is presented to the direction of loading, ensuring that maximum anchor capacity is achievable through bearing resistance. The anchor concept including the installation and keying processes are shown schematically on Figure 6.

Work at the CGSE on the DEPLA includes centrifuge and reduced scale field tests, analytical modelling and three-dimensional large deformation finite element analyses. The centrifuge and field tests (O'Loughlin *et al*., 2014a) indicate that installation behaviour for DEPLAs is similar to other dynamically installed anchors, with final tip embedments of between 2 and 3 times the anchor length in normally consolidated clay. As anchor capacity is controlled by the local strength at the final anchor embedment depth, reliability in anchor capacity is governed to a large degree by the success in predicting the anchor embedment depth after dynamic installation. This may be calculated empirically using a total energy approach, or more rigorously by considering the forces acting on the anchor during dynamic embedment and calculating the net acceleration on the anchor in a time stepping fashion. This aspect is considered in detail by O'Loughlin *et al*. (2014b) in a separate paper within this special issue.

A full-scale DEPLA suited to mobile operations in a site with a seabed strength profile of $s_u = 1.5z$ kPa, where z is the depth below mudline, would be about 10 m high, with a follower mass of 36 tonnes and a plate mass of 30 tonnes. For this scale, the anchor terminal velocity would be between 25 and 30 m/s (depending on the release line configuration), with a final (keyed) plate anchor embedment depth of 18 m (4.5 times the plate diameter).

Mobilising capacity for the DEPLA follows the same procedure as for the SEPLA and other plate anchors that are installed in a vertical orientation. Upon loading, the anchor keys to develop its maximum bearing capacity, losing embedment in the process. The anchor trajectory, and in particular the loss of embedment during the keying process, can be estimated using the same techniques developed for the SEPLA. However, the cruciform plate geometry of the DEPLA is evidently quite different from the SEPLA, and it is expected that the combined vertical, horizontal and moment yield envelope will differ from those established for the SEPLA, particularly as other fluke geometries are considered in an attempt to optimise the DEPLA geometry (Wang and O'Loughlin, 2014). Work in progress includes development of such envelopes for a variety of fluke configurations. These envelopes will be incorporated in the CASPA prediction tool (Cassidy *et al*., 2012) to establish the optimal DEPLA plate geometry from a (post-keying) capacity perspective.

The DEPLA concept was developed and proven through a series of centrifuge and field trials by the CGSE. The success of this testing campaign resulted in a commercial deal between the UWA node of the CGSE and Vryhof Anchors, who now have full and exclusive rights to the DEPLA technology and are continuing to work with the CGSE to continue the development pipeline, culminating with full-scale field trials.

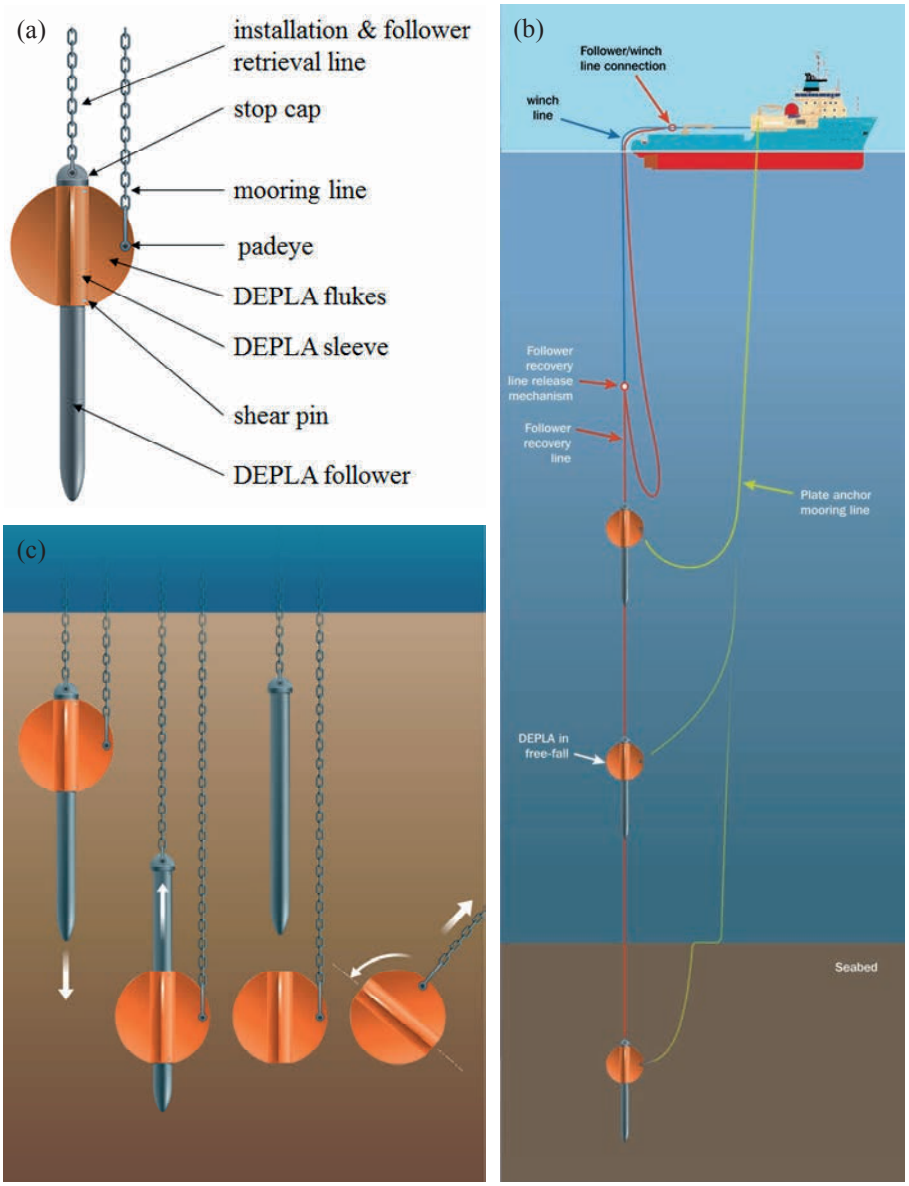

Figure 6: Dynamically embedded plate anchor: (a) annotated schematic, (b) installation procedure, (c) post installation keying and capacity mobilisation.

4.2 DEPLA CAPACITY

Prediction of the (DEPLA) plate anchor capacity firstly requires successful prediction of the final embedment depth. Work by the CGSE on this aspect of the problem is summarised in O'Loughlin *et al*. (2014b) (this issue). The following summarises work in the Centre on keying and capacity mobilisation.

Example plate anchor keying and capacity curves from centrifuge DEPLA tests reported by O'Loughlin *et al*. (2014a) are provided on Figure 7 for a square and circular plate anchor installed both dynamically and statically and subjected to pure vertical loading. Anchor resistance on Figure 7 is normalised by the area of the plate, A, and the undrained shear strength at the estimated anchor embedment at peak capacity, $s_{u,p}$, whereas the vertical displacement of the anchor padeye is normalised by either the diameter, D, or breadth, B, of the plate anchor for circular and square plates, respectively. In the main, the load-displacement responses in Figure 7 are typical of those observed experimentally for plate anchors (e.g. Song *et al.,* 2006; Gaudin *et al*., 2006; Blake *et al*., 2010), with an initial stiff response as the anchor begins to rotate, followed by a softer response as the rotation angle increases and a final stiff response as the anchor capacity is fully mobilised. The range in the bearing capacity factor $N_c = (F_v – W_s)/As_{u,p}$, which adjusts for the peak force by the submerged weight of the anchor, W_s, is also indicated on Figure 7, and is in the range 14.2 to 17.3 with an arithmetic mean $N_c = 15$. Corresponding plate anchor keying and capacity curves from field tests at scales between 1:12 and 1:4.5 using a DEPLA with circular flukes are shown on Figure 8 and compared with a typical result from the

centrifuge tests. The response in both the field tests and the centrifuge tests is qualitatively consistent, with N_c = 14.5 to 15.7 in the field tests, compared with the arithmetic mean N_c = 15 from the centrifuge tests. However, the loss in embedment is significantly higher in the field tests, as reflected in the much softer-load displacement response. The reason for this is not clear and will be investigated in further field trials at the CGSE National Soft Soil Field Testing Facility in Ballina, NSW as described in Kelly *et al*. (2014) (this issue).

In Figure 9, the experimental data from the centrifuge and field tests are compared with the corresponding solutions for a vanishingly thin circular plate anchor, which are N_c = 12.42 and 13.11 for smooth and rough plates respectively (Martin and Randolph, 2001). These solutions underestimate the capacity of anchors with finite plate thickness (Wang *et al.,* 2010a). Wang and O'Loughlin (2014) conducted three-dimensional large deformation finite element analyses of the DEPLA plate configurations used in the centrifuge tests. The results from these analyses are also shown on Figure 9, where good agreement with the experimental data can also be observed.

The transition from shallow to deep failure mechanisms within the soil, as established from the numerical analyses, is shown in Figure 10, which plots the capacity factor N_c at different normalised embedment depths and for different load inclinations. For practical purposes the transitional embedment depth between shallow and deep behaviour could be established at H/D = 2.5, with a reduction in capacity factor at shallower embedments, particularly as the load inclination becomes more inclined. Hence, a DEPLA design should aim for a final plate embedment depth in excess of 2.5 diameters; this is quite achievable in normally consolidated soils with strength gradients in the range of k = 1 to 2 kPa/m.

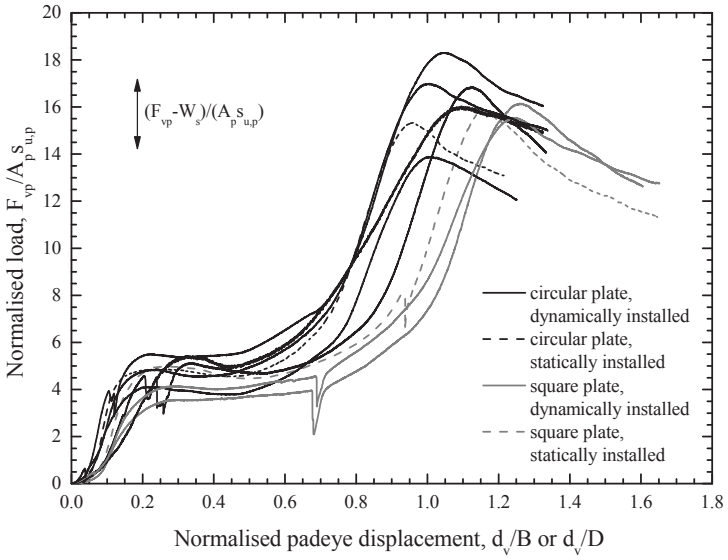

Figure 7: Dimensionless load-displacement response during DEPLA centrifuge tests.

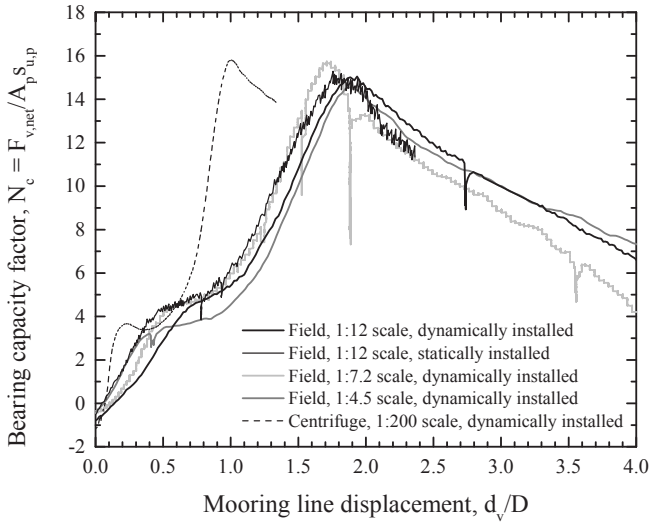

Figure 8: Comparison of field and centrifuge load-displacement response.

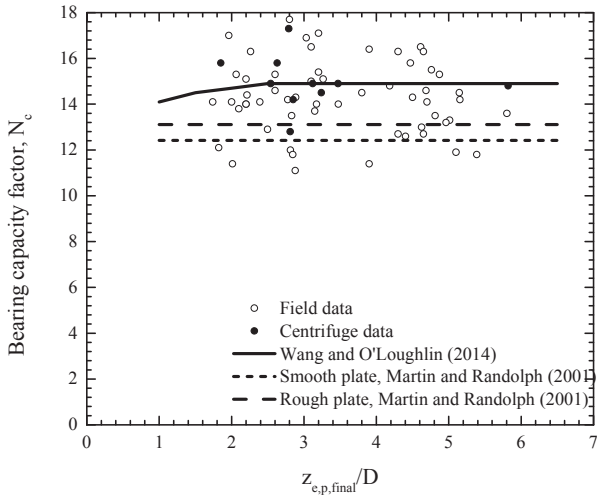

Figure 9: Comparison of experimental and numerical anchor capacity factors.

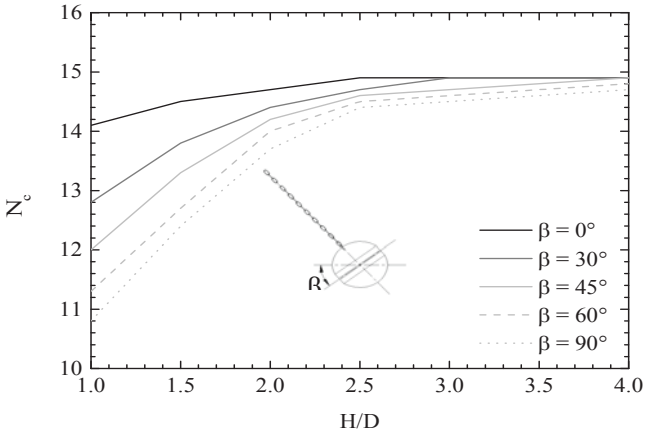

Figure 10: Variation of DEPLA capacity factor at different embedment depths and plate inclinations.

5 HELICAL ANCHORS

Helical anchors, also known as helical piles, are screw-type foundations consisting of a series of multiple helical plates affixed to a central shaft. The helical plates serve not only to provide most of the capacity to resist uplift and bearing forces following installation but also to propel the anchor as it is twisted into the ground. The installation method offers distinct advantages over traditional deep foundations, especially with respect to versatility and cost effectiveness. These advantages, combined with an increasing level of familiarity in the geotechnical community, have caused a dramatic rise in popularity in recent decades (Perko, 2009).

Compared to single-plate anchors, the difficulty in understanding and predicting the behaviour of multi-plate anchors is compounded by potential interaction between the plate elements, which is oversimplified in the prevailing methods for predicting ultimate uplift capacity. The two most common methods are known as the 'individual bearing method' and the 'cylindrical shear method' (Perko, 2009). The individual bearing method assumes that each helical plate contributes a resistance that can be evaluated using the Terzaghi-Meyerhof bearing capacity formula. The cylindrical shear method postulates that resistance derives from the sum of the bearing capacity of the uppermost plate (again determined using the Terzaghi-Meyerhof formula) and the shear resistance along the cylinder of soil passing through the edges of each plate. In practice, calculations are completed using both methods, and the smaller of the predicted capacities is then utilised for design purposes.

Work within the CGSE has focused on developing a rigorous framework for predicting the undrained uplift capacity of multi-plate anchors based on a thorough understanding of the failure mechanisms involved. Figure 11 exemplifies the work of Merifield and Smith (2010), Merifield (2011) and Wang *et al*., 2013(b), who completed a large number of simulations based on various methods, including numerical limit analysis and finite element analysis, to show variations

in the failure mechanism and uplift capacity as a function of the embedment depth ratio H/D, the plate spacing ratio S/D, and the total number of plates. The figure highlights the transition in the failure mechanism as the spacing ratio S/D varies. For closely spaced plates (small S/D), the failure mechanism extends between plates (Figure 11a), and as the spacing ratio increases, the mechanism dissociates into localised failure mechanisms (Figure 11c). Based on small-strain finite element analysis, Merifield (2011) identified a critical spacing ratio of $S/D \approx 1.6$ at which the transition occurs, and simple design equations that display favourable agreement with available laboratory data were also developed. In a subsequent study, Wang *et al*., (2013b) completed a series of analyses using a large deformation finite element (LDFE) approach, and their results suggested a larger value for the critical spacing ratio, $S/D \approx 3.2$. The difference attests to the complexity of the interaction between plates and can be ascribed to variations in the analysis type (small versus large deformation) and the different contact conditions assumed at the soil-anchor interfaces (smooth versus rough). Both values fall within the range of critical spacing ratios inferred from laboratory testing, $1.5 < S/D < 3.4$ (Perko, 2009). Ongoing work within the CGSE focuses on developing a unified design framework that accounts for all of the factors that influence uplift capacity, including the contact conditions, plate geometry (e.g., thickness) and, perhaps most importantly, the shaft.

Centrifuge tests completed within the CGSE have revealed additional insights into the response of helical anchors to uplift loading, especially with respect to the character of the force-displacement relationship and the effects of installation. In a series of tests aimed at investigating different combinations of plate spacing and embedment depth for helical anchors in single-, dual- and triple-plate configurations, Wang *et al*., (2010b) and Wang *et al*. (2013b) showed that the post-peak (softening) response depends on the anchor configuration. In particular, the study revealed that single-plate anchors exhibit a more ductile response than multi-plate systems, which may be beneficial in reducing the likelihood of progressive failure in systems relying on multiple helical anchors. The latter study also demonstrated the impact of the installation process on capacity. For multi-plate anchors, predictions of uplift capacity obtained using an estimate of the remoulded shear strength were found to be closer to the measured uplift capacities compared to predictions based on the intact shear strength, where the remoulded strength was roughly 70% of the intact strength. On the other hand, the intact shear strength was found to be more appropriate for single-plate anchors, which tend to disturb the soil less during installation. Additional details concerning the effects of installation are given in a companion paper in this issue devoted to modelling the installation process (Hambleton *et al*., 2014).

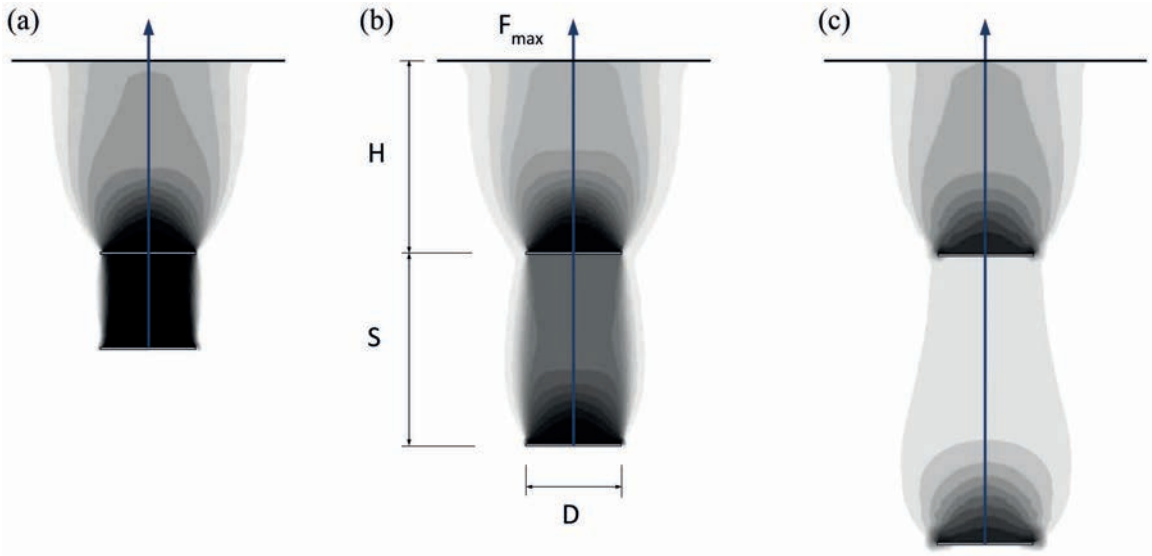

Figure 11: Variations in the failure mechanism for undrained uplift of a dual-helix anchor with an embedment ratio H/D = 2 and different values of the spacing ratio S/D: (a) S/D = 1, (b) S/D = 2; (b) S/D = 3 (adapted from Merifield, 2011).

6 CONCLUSIONS AND PERSPECTIVES

The paper illustrates some of the challenges raised by anchor-soil interaction and anchor performance, as well as the advances achieved by the CGSE both in terms of realistic modelling techniques and understanding the fundamental aspects governing anchor behaviour. Significant work is still being undertaken on dynamically penetrated anchors and helical anchors, as highlighted in O'Loughlin *et al*. (2014) and Hambleton *et al*. (2014), respectively (see papers in this special issue). The main focus is on installation effects and strength recovery on the subsequent anchor capacity. In parallel, a new research field is being investigated, which relates to anchoring systems for floating renewable energy devices (e.g. wind turbines and wave energy converters). While some of the existing technology and knowledge from

anchoring systems for oil and gas platforms can be transferred, some specific new challenges need to be addressed. They are notably associated with multidirectional loadings (as anchors are shared by multiple devices arranged in array), installation in soil with complex stratigraphy (as commonly encountered in shallow waters), and the wide range of loads applied to the anchor, which can span 2 orders of magnitude (from ~ 200 kN to ~ 20 MN). This work will benefit from the experimental facilities underway within the CGSE and presented in Kelly *et al.* (2014) and Cassidy *et al*. (2014) (see papers in this special issue) and the synergy between the three nodes of the CGSE.

7 ACKNOWLEDGEMENTS

This work forms part of the activities of the Centre for Offshore Foundation Systems (COFS), currently supported as a node of the Australian Research Council Centre of Excellence for Geotechnical Science and Engineering.

8 REFERENCES

Blake A., O'Loughlin C.D., Gaudin, C. (2010). Setup following keying of plate anchors assessed through centrifuge tests in kaolin clay. *Proceedings of the 2nd International Symposium on Frontiers in Offshore Geotechnics, ISFOG2010*, Perth, Australia, 705-710.

Cassidy M.J., Gaudin C., Randolph M.F., Wong P.C., Wang D., Tian Y. (2012). A plasticity model to assess the keying behaviour and performance of plate anchors. *Géotechnique*. 62(9): 825-836.

Cassidy M.J., Gaudin C., Bates L., Indraratna B., Nimbalkar S., O'Loughlin C.D., White D.J., Sloan S.W. (2014). Advancing Australia's facilities for physical modelling in geotechnics. *Australian Geomechanics*, 49(4), 3-14.

Dove P., Tre, H., Wilde, B. (1998). Suction embedded plate anchor (SEPLA): a new anchoring solution for ultra-deepwater mooring. *Deep offshore technology conference*.

Ehlers C. J., Young A. G., Chen J. H. (2004). Technology assessment of deepwater anchors. *Offshore Technology Conference*. OTC 16840.

Elkhatib S. (2006). *The behaviour of drag-in plate anchors in soft cohesive soils*. PhD Thesis. The University of Western Australia.

Gaudin C., O'Loughlin C.D., Randolph M.F., Lowmass, A. (2006). Influence of the installation process on the performance of Suction Embedded Plate Anchors. *Géotechnique*, 56(6), 389-391.

Gaudin C., Tham K.H., Ouahsine S. (2008). Plate anchor failure mechanism during keying process. *18th Inernational Offshore and Polar Engineering Conference*, Vancouver, Canada. 2: 613-620.

Gaudin C., Simkin M., White D.J., O'Loughlin C.D. (2010c). Experimental investigation into the influence of a keying flap on the keying behaviour of plate anchors. *20th Inernational Offshore and Polar Engineering Conference*, Beijing, China.

Hambleton J.P., Stanier S.A., Gaudin C., Todeshkejoei K. (2014). Analysis of installation forces for helical piles in clay. *Australian Geomechanics*, 49(4), 73-80.

Han C., Wang D., Gaudin C., Cassidy M.J., O'Loughlin C.D. (2015). Soil flow mechanism around horizontal plate anchors during monotonic and sustained loadings. *3rd International Conference on Frontiers in Offshore Geotechnics*, Oslo Norway.

Kelly R., O'Loughlin C.D., Bates L., Gourvenec S.M., Colreavy C., White D.J., Gaone F.M., Doherty J.P., Randolph M.F. (2014). In situ testing at the National Soft Soil Field Testing Facility, Ballina, New South Wales. *Australian Geomechanics*, 49(4), 15-26.

Martin C.M. and Randolph M.F. (2001). Applications of the lower and upper bound theorems of plasticity to collapse of circular foundations. *10th International Conference of the International Association for Computer Methods and Advances in Geomechanics*, Tucson, USA. 2: 1417-1428.

Merifield R.S. (2011). The ultimate uplift capacity of multi-plate helical type anchors in undrained clay. *Journal of Geotechnical and Geoenvironmental Engineering*, 137(7): 704-716.

Merifield R.S., Lyamin A.V., Sloan S.W. (2005). Stability of inclined strip anchors in purely cohesive soil. *Journal of Geotechnical and Geoenvironmental Engineering,* 131, 792-799.

Merifield R.S., Lyamin A.V., Sloan S.W. (2006). Three-dimensional lower-bound solutions for the stability of plate anchors in sand. *Géotechnique*, 56(2), 123-132.

Merifield R.S., Lyamin A.V., Sloan S.W., Yu H.-S. (2003). Three-dimensional lower bound solutions for stability of plate anchors in clay. *Journal of Geotechnical and Geoenvironmental Engineering*, 129, 243-253.

Merifield R.S., Sloan S.W. (2006). The ultimate pullout capacity of anchors in frictional soils. *Canadian Geotechnical Journal*, 43, 852-868.

Merifield R.S., Sloan S.W., Yu H.-S. (2001). Stability of plate anchors in undrained clay. *Géotechnique*, 51, 141-153.

Merifield, R.S., Smith, C.C. (2010). The ultimate uplift capacity of multi-plate strip anchors in undrained clay. *Computers and Geotechnics*, 37: 501-514.

O'Loughlin C.D., Lowmass A., Gaudin C.D., Randolph M. F. (2006). Physical modelling to assess keying characteristics of plate anchors. *Proc. 7th International Conference on Physical Modelling in Geotechnics*, Hong Kong. 1: 659-665.

O'Loughlin C.D., Blake A., Richardson M.D., Randolph M.F., Gaudin, C. (2014a). Installation and capacity of dynamically embedded plate anchors as assessed through centrifuge tests. *Ocean Engineering*, 88, 204-213.

O'Loughlin C.D., Nazem N., Chow S.H., Randolph M.F., Gaudin C., White D.J. (2014b). Dynamic embedment of projectiles in clay. *Australian Geomechanics*, 49(4), 133-146.

Perko H.A. (2009). *Helical Piles, A practical Guide to Design and Installation*. Hoboken. New Jersey: John Wiley & Sons, Inc.

Song Z., Hu, Y., O'Loughlin C.D. (2006). Anchor and chain reaction during inclined pullout in clay. *Proceedings of the 25th International Conference on Offshore Mechanics and Arctic Engineering*, Hamburg, Germany, OMAE2006-92411.

Song Z., Hu Y., Randolph M.F. (2008). Numerical simulation of vertical pullout of plate anchors in clay. *Journal of Geotechnical and Geoenvironmental Engineering,* ASCE. 134(6): 866-875.

Song Z., Hu Y, O'Loughlin C.D., Randolph M.F. (2009). Loss in anchor embedment during plate anchor keying in clay. *Journal of Geotechnical and Geoenvironmental Engineering,* ASCE. 135(10): 1475-1485.

Tian Y., Gaudin C., Cassidy M.J., Randolph M.F. (2013). Considerations on the Design of Keying Flap of Plate Anchors. *Journal of Geotechnical and Geoenvironmental Engineering*, ASCE. 139(7): 1156-1164.

Tian Y., Gaudin C., Randolph, M.F., Cassidy M.J. (2014a). The influence of padeye offset on the bearing capacity of three dimensional plate anchors. *Canadian Geotechnical Journal.* DOI: 10.1139/cgj-2014-0120.

Tian Y., Gaudin C., Cassidy M.J. (2014b). Improving plate anchor design with a keying flap. *Journal of Geotechnical and Geoenvironmental Engineering*, ASCE 140(5): 04014009.

Tian Y., Cassidy M.J., Gaudin C. (2014c). The influence of the padeye offset on the plate anchor re-embedding behaviour. *Géotechnique Letters*. 4: 39-44.

Wang D., Hu Y., Randolph M.F. (2010a). Three-dimensional large deformation finite element analysis of plate anchors in uniform clay. *Journal of Geotechnical and Geoenvironmental Engineering*, ASCE. 136(2): 355-365.

Wang D., Merifield R.S., Gaudin C., Hu Y. (2010b). Centrifuge model tests of helical anchors in clay. *7th International Conference on Physical Modelling in Geotechnic*s, Zurich, Switzerland.1: 1069-1074.

Wang D., Hu Y., Randolph, M.F. (2011). Keying of rectangular plate anchors in normally consolidated clays. *Journal of Geotechnical and Geoenvironmental Engineering,* ASCE. 137(12): 1244-1253.

Wang D., Gaudin C., Randolph M.F. (2013a). Large deformation finite element analysis investigating the performance of anchor keying flap. *Ocean Engineering*. 59(1): 107-116.

Wang D., Merifield R.S., Gaudin, C. (2013b). Uplift behaviour of helical anchors in clay. *Canadian Geotechnical Journal*. 50: 575-584.

Wang D., O'Loughlin, C.D. (2014). Numerical study of pull-out capacities of dynamically embedded plate anchors. *Canadian Geotechnical Journal*. DOI: 10.1139/cgj-2013-0485.

Wilde B., Treu H., Fulton, T. (2001). Field testing of suction embedded plate anchors. *11th International Offshore and Polar Engineering Conference*. 544-551.

Wong P., Gaudin C., Randolph M. F., Cassidy M. J., Tian Y. (2012) Performance of suction embedded plate anchors in permanent mooring applications. *22nd International Offshore and Polar Engineering Conference,* Greece. 2: 640-645.